

# <sup>90</sup>Nb – a potential PET nuclide: production and labeling of monoclonal antibodies

By V. Radchenko<sup>1</sup>, H. Hauser<sup>2</sup>, M. Eisenhut<sup>2</sup>, D. J. Vugts<sup>3,4</sup>, G. A. M. S. van Dongen<sup>3,4</sup> and F. Roesch<sup>1,\*</sup>

<sup>1</sup> Institute of Nuclear Chemistry, Johannes Gutenberg-University Mainz, Fritz-Straßmann-Weg 2, 55128 Mainz, Germany

<sup>2</sup> Radiopharmaceutical Chemistry, German Cancer Research Center, Im Neuenheimer Feld 280, 69120 Heidelberg, Germany

<sup>3</sup> VU University Medical Center, Dept. of Nuclear Medicine and PET Research, De Boelelaan 1085 c, Amsterdam, The Netherlands

<sup>4</sup> VU University Medical Center, Dept. of Otolaryngology/Head and Neck Surgery, De Boelelaan 1117, Amsterdam, The Netherlands

(Received September 21, 2011; accepted in revised form January 25, 2012)

(Published online April 10, 2012)

*Immuno-PET / Niobium-90 / Radiolabeling /  
Desferrioxamine / Monoclonal antibodies /  
p-isothiocyanatobenzyl-desferrioxamine /  
TFP-N-succinyl-desferrioxamine*

**Summary.** Fast progressing *immuno*-PET gives reasons to develop new potential medium-long and long-lived radioisotopes. One of the promising candidates is <sup>90</sup>Nb. It has a half-life of 14.6 h, which allows visualizing and quantifying processes with medium and slow kinetics, such as tumor accumulation of antibodies and antibodies fragments or polymers and other nanoparticles. <sup>90</sup>Nb exhibits a high positron branching of 53% and an optimal energy of  $\beta^+$  emission of  $E_{\text{mean}} = 0.35$  MeV only. Consequently, efficient radionuclide production routes and Nb<sup>V</sup> labeling techniques are required.

<sup>90</sup>Nb was produced by the <sup>90</sup>Zr(p,n)<sup>90</sup>Nb nuclear reaction on natural zirconium targets. No-carrier-added (n.c.a.) <sup>90</sup>Nb was separated from the zirconium target *via* a multi-step separation procedure including extraction steps and ion-exchange chromatography. Protein labeling was exemplified using the bifunctional chelator desferrioxamine attached to the monoclonal antibody rituximab. Desferrioxamine was coupled to rituximab *via* two different routes, by the use of N-succinyl-desferrioxamine (N-suc-Df) and by means of the bifunctional derivative *p*-isothiocyanatobenzyl-desferrioxamine B (Df-Bz-NCS), respectively. Following antibody modification, labeling with <sup>90</sup>Nb was performed in HEPES buffer at pH 7 at room temperature. *In vitro* stability of the radiolabeled conjugates was tested in saline buffer at room temperature and in fetal calf serum (FCS) at 37 °C.

The selected production route led to a high yield of  $145 \pm 10$  MBq/ $\mu$ A h of <sup>90</sup>Nb with high radioisotopic purity of > 97%. This yield may allow for large scale production of about 10 GBq <sup>90</sup>Nb. The separation procedure resulted in 76–81% yield. The Zr/<sup>90</sup>Nb decontamination factor reaches 10<sup>7</sup>. Subsequent radiolabeling of the two different conjugates with <sup>90</sup>Nb gave high yields; after one hour incubation at room temperature, more than 90% of <sup>90</sup>Nb-Df-mAb was formed in both cases. At room temperature in aqueous solution, both <sup>90</sup>Nb-Df-mAb constructs were more than 99% stable over a period of 18 d.

The developed production and separation strategy provided <sup>90</sup>Nb with purity appropriate for radiolabeling applications.

\* Author for correspondence (E-mail: frank.roesch@uni-mainz.de).

Labeling and stability studies proved the applicability of <sup>90</sup>Nb as a potential positron emitter for *immuno*-PET.

## 1. Introduction

A variety of antibodies and antibody fragments for different targets of interest is currently under preclinical investigation [1]. Although a rather low number of all developed antibodies make it to a worldwide use in clinics, 28 different antibodies are approved by the US Food and Drug Administration today [2]. One such approved antibody is rituximab (the first monoclonal antibody approved for the treatment of lymphoma), a genetically engineered monoclonal chimeric antibody, targeting the CD20 antigen expressed on B cells [3]. To improve the evaluation of potential new antibodies and to facilitate the transfer of candidates into the clinic, *immuno*-PET may be applied [4]. Since the 1990s, several positron emitting radionuclides with long and medium half-lives have been tested for their applicability in *immuno*-PET, for recent reviews *cf.* [5–7]. Antibodies with blood-clearance half-lives of days to weeks call for radionuclides with corresponding half-lives to enable *immuno*-PET scans at, for example, 7–9 d p.i. Consequently, commercially available and established positron emitters for the imaging peptides and proteins with slow pharmacokinetics are <sup>86</sup>Y ( $T_{1/2} = 14.7$  h), <sup>89</sup>Zr ( $T_{1/2} = 78.4$  h) and <sup>124</sup>I ( $T_{1/2} = 100.2$  h). Nuclear data are summarized in Table 1. One example of application of <sup>89</sup>Zr is the use of ibritumomab tiuxetan (Zevalin<sup>®</sup>) [8] labeled with <sup>89</sup>Zr and the development of <sup>89</sup>Zr-labeled U36, a chimeric antibody specific for CD44v6 [9]. These results already demonstrate the potential of <sup>89</sup>Zr in *immuno*-PET with intact antibodies. *Immuno*-PET imaging with <sup>124</sup>I-cG250 (anticarbonic anhydrase-IX) resulted in successful detection of 15 of 16 clear-cell carcinomas [10]. However, those antibodies do not provide optimal imaging properties. The long lasting circulation and the very slow kinetics necessitate long delays between administration of the radiotracer and the acquisition of the final PET imaging.

For faster pharmacokinetics, antibodies fragments have been developed [11, 12]. As a result, their enhanced clearance

**Table 1.** Decay characteristics of several PET radionuclides relevant to *immuno*-PET imaging (with increasing  $T_{1/2}$ ), taken from [16] unless otherwise stated.

Radionuclide	Half-life h	Main production route <sup>a</sup>	$E_{\beta^+}$ mean in MeV ( $\beta^+$ yields)	Most intensive $\gamma$ -emissions in MeV (abundance)
<sup>64</sup> Cu	12.7	<sup>64</sup> Ni( $p, n$ ) <sup>64</sup> Cu <sup>64</sup> Ni( $d, 2n$ ) <sup>64</sup> Cu	0.05 (17.8%) [17] (accompanied $\beta^-$ , $E_{\beta^-}$ mean 0.075 MeV (38.4%))	1.345 (0.54%) [17]
<sup>90</sup> Nb	14.6	<sup>90</sup> Zr( $p, n$ ) <sup>90</sup> Nb	0.35 (53.0%)	0.14 (66.7%) 1.13 (92.0%) 2.32 (82.0%)
<sup>86</sup> Y	14.7	<sup>86</sup> Sr( $p, n$ ) <sup>86</sup> Y	0.22 (33.0%)	0.63 (32.6%) 1.08 (83.0%) 1.15 (30.5%)
<sup>76</sup> Br	16.2	<sup>76</sup> Se( $p, n$ ) <sup>76</sup> Br <sup>75</sup> As( $^3$ He, $2n$ ) <sup>76</sup> Br	0.64 (58.2%) [17]	0.55 (74.0%) 0.66 (15.9%) 1.85 (14.7%)
<sup>89</sup> Zr	78.4	<sup>89</sup> Y( $p, n$ ) <sup>89</sup> Zr <sup>89</sup> Y( $d, 2n$ ) <sup>89</sup> Zr	0.09 (23.0%)	0.91 (100.0%) 1.71 (0.76%) 1.74 (0.13%)

a: For a review [cf. 6, 7].

dramatically reduces the interval between radiotracer injection and the actual imaging to hours instead of days. For imaging with engineered antibody fragments radionuclides with medium half-lives are required, for example <sup>64</sup>Cu ( $T_{1/2} = 12.7$  h) [13], <sup>86</sup>Y ( $T_{1/2} = 14.7$  h) [14], <sup>76</sup>Br ( $T_{1/2} = 16.2$  h) [15]. Their decay data are given in Table 1 [16, 17].

Several crucial factors and characteristics apply to radionuclides for *immuno*-PET. The most important factors are: i) a physical half-life paralleling the biological half-life of the antibody or antibody fragment; ii) a preferably low  $\beta^+$ -energy to allow high-resolution PET imaging; iii) a high positron branching with no or weak accompanying irradiation ( $\beta^-$ ,  $\gamma$ ) to offer high-sensitive PET imaging while reducing the radiation burden of the patient and iv) the availability of the radionuclide, *i.e.* an efficient production route.

In this study, <sup>90</sup>Nb is proposed for *immuno*-PET. Its intermediate half-life of 14.6 h appears appropriate for antibody fragments as well as for antibodies. Another advantage of <sup>90</sup>Nb is its decay parameters. Its positron branching is as high as 53% at rather low  $\beta^+$ -energy of  $E_{\text{mean}} = 350$  keV ( $E_{\text{max}} = 1.5$  MeV) (Table 1), which should allow high resolution images.

Continuing our initial work on the production and radiochemical separation of <sup>90</sup>Nb [18, 19], and systematic studies on using desferrioxamine for <sup>90</sup>Nb labeling [20], this work aims to explore parameters of <sup>90</sup>Nb-Df-mAb labeling and stability. Recently, new synthetic approaches towards conjugation of desferrioxamine (Df) derivatives to monoclonal antibodies have been described in the context of <sup>89</sup>Zr<sup>IV</sup>-*immuno*-PET [21, 22]. This chemistry appears promising also for <sup>90</sup>Nb<sup>V</sup>. Consequently, a monoclonal antibody was selected for <sup>90</sup>Nb-labeling utilizing two different strategies of covalently binding Df to the protein.

## 2. Materials and methods

### 2.1 Materials

Reagents were purchased from Sigma-Aldrich (Germany) and used without further purification, unless otherwise stated. Deionized water ( $18 \text{ M}\Omega \text{ cm}^{-1}$ ) and ultra-pure HCl solution were used. No further special measures were taken regarding working under strict metal-free conditions. The mAb rituximab (MabThera<sup>®</sup>, 10 mg/mL) directed against CD20 was bought from Roche Nederland BV (Woerden, The Netherlands). For purification of conjugated and labeled antibodies, PD-10 columns (GE Healthcare Life Science) were applied, for anion exchange separation Aminex A27,  $15 \pm 2 \mu\text{m}$ , anionic exchange resin (BioRad) was used.

The production yield, radionuclidic purity, radiochemical purity and separation yield of <sup>90/95</sup>Nb were determined by  $\gamma$ -ray spectroscopy using an Ortec HPGe detector system and Canberra Genie 2000 software. The dead time of the detector was always kept below 10%. The detector was calibrated for efficiency at all positions with the certified standard solution QCY48, R6/50/38 (Amersham, UK).

### 2.2 Production of <sup>90</sup>Nb and <sup>95</sup>Nb

<sup>90</sup>Nb was produced *via* the <sup>90</sup>Zr( $p, n$ )<sup>90</sup>Nb reaction at the cyclotron MC32NI of the German Cancer Research Center, Heidelberg. For irradiation, a stack of three discs of natural zirconium (natural abundance: 51.45% <sup>90</sup>Zr) foils of 10 mm diameter and a thickness of 0.25 mm each was used (Fig. 1). Irradiation was performed at 20 MeV proton energy and a current of 5  $\mu\text{A}$  for 1 h. This initial proton energy decreased, by using an aluminum holder cover of 0.5 mm thickness, to 17.5 MeV while entering the first foil of Zr. 24 h after end of irradiation (EOB), production yield and impurities were measured by gamma ray spectroscopy.

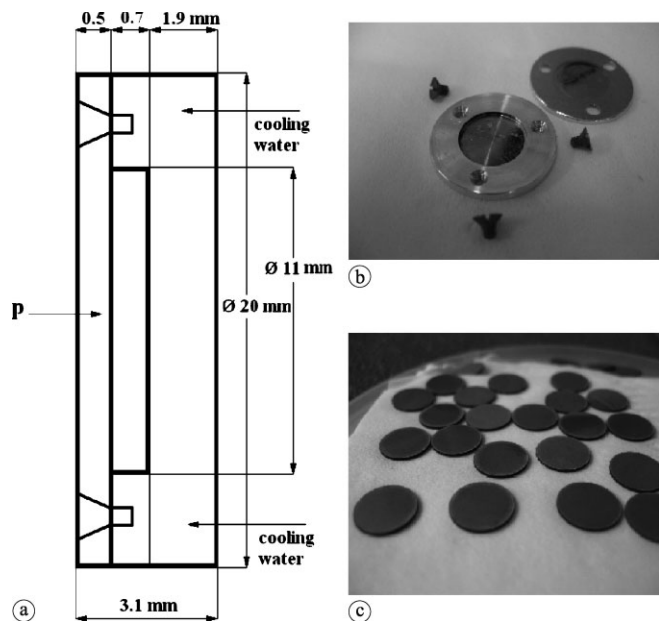


**Fig. 1.** Irradiation setup. (a) Schematic view of the target holder (profile). (b) Open target holder (full face) with aluminum cover. (c) Natural zirconium discs for irradiation ( $\varnothing 10$  mm, 0.25 mm thickness).

The absolute activity of <sup>90</sup>Nb was calculated as average of its two gamma-lines at 141.2 keV (66.8% abundance) and 1129.2 keV (92.7%). The irradiation yield of <sup>90</sup>Nb was calculated as the mean of three irradiations.

<sup>97</sup>Nb ( $T_{1/2} = 74$  min) and <sup>95</sup>Nb ( $T_{1/2} = 35$  d) were employed for the development of the separation chemistry (as well as determination of the decontamination factor and testing purposes). <sup>97</sup>Nb was produced *via* the <sup>96</sup>Zr( $n, \gamma$ )  $\rightarrow$  <sup>97</sup>Zr( $\beta^-$ ,  $T_{1/2} = 16.9$  h)  $\rightarrow$  <sup>97</sup>Nb reaction and <sup>95</sup>Nb was produced *via* the <sup>94</sup>Zr( $n, \gamma$ )  $\rightarrow$  <sup>95</sup>Zr( $\beta^-$ ,  $T_{1/2} = 64$  d)  $\rightarrow$  <sup>95</sup>Nb reaction from natural zirconium granules (1–3 mm, 99.8% ChemPur, Germany). Neutron irradiations were performed at the TRIGA reactor at the University of Mainz, Germany, and at the research reactor BERII at the Helmholtz Center Berlin, Germany. In the latter case 300 mg were irradiated at a neutron flux of  $2 \times 10^{14} \text{ s}^{-1} \text{ cm}^{-2}$  (BER II) for 50 d and more than 1.5 GBq of <sup>95</sup>Zr was obtained. Production of both isotopes, <sup>95</sup>Zr and <sup>95</sup>Nb, was monitored by gamma ray spectroscopy, *via* emissions at 724.2 keV (44.2%) and 756.7 keV (54.0%) for <sup>95</sup>Zr and *via* the 765.8 keV (100%) for <sup>95</sup>Nb. <sup>97</sup>Zr was monitored by gamma emission at 743.4 keV (93.0%) and <sup>97</sup>Nb at 658.1 keV (98.0%). The maximum daughter activity of <sup>95</sup>Nb generated from <sup>95</sup>Zr was obtained at  $\sim 67$  d, EOB.

### 2.3 Separation and purification of n.c.a. <sup>90/95</sup>Nb

The separation procedure was modified following the procedure described by Busse *et al.* [19]. In short, the zirconium metal target ( $260 \pm 3$  mg) was transferred into a 50 mL vial and 2 mL of water were added. Under ice-cooling, 48% HF (0.63 mL) was added in small portions. After complete dissolution, 10 M HCl (6 mL) and saturated boric acid (3.4 mL) were added. The <sup>90/95</sup>Nb fraction was extracted with 0.02 M *N*-benzoyl-*N*-phenylhydroxylamine (BPHA) in CHCl<sub>3</sub> (5 mL) by vigorous stirring of the two phases in a 50 mL vial for 20 min. The aqueous phase was additionally

washed with CHCl<sub>3</sub> (3 mL). The organic phases were combined and washed with a mixture of 9 M HCl/0.001 M HF (2 mL) and with 9 M HCl (2 mL) and finally extracted with aqua regia (5 mL).

For a final purification of <sup>90/95</sup>Nb from remaining trace amounts of zirconium, an anionic exchange method was employed. After aforementioned back extraction, the aqueous phase was evaporated to dryness. The residue was dissolved in a mixture of 0.25 M HCl/0.1 M oxalic acid (0.5 mL) and adsorbed on a small Aminex A27,  $15 \pm 2 \mu\text{m}$ , anionic exchange column ( $20 \times 1.5$  mm). Elution was performed under slight overpressure of 0.3 bars. After loading, the column was washed with 10 M HCl (100  $\mu\text{L}$ ). Residues of Zr were removed by washing with a mixture of 9 M HCl/0.001 M HF (200  $\mu\text{L}$ ). <sup>90/95</sup>Nb was eluted by a mixture of 6 M HCl/0.01 M oxalic acid (200  $\mu\text{L}$ ).

### 2.4 Preparation of TFP-N-suc-Df-mAb

Conjugation of TFP-N-suc-Df to rituximab (MabThera<sup>®</sup>) was performed at VU University Medical Center, Amsterdam. Conjugation follows the multi-step procedure as previously described [21] (Fig. 2). In short, the chelate Df was succinylated (N-suc-Df), temporarily filled with stable iron Fe<sup>III</sup>, and coupled to the lysine residues of rituximab (5 mg/mL) by means of a tetrafluorophenol-N-suc-Df ester. After removal of Fe<sup>III</sup> by trans-chelation to EDTA at 35 °C, the modified mAb was purified on a PD-10 column using normal saline as eluent.

### 2.5 Preparation of Df-Bz-NCS-mAb

Df-Bz-NCS was purchased from Macrocyclics. Rituximab was modified with Df-Bz-NCS as illustrated in Fig. 3 [22]. In short, while gently shaking, a threefold molar excess of Df-Bz-NCS (in 20  $\mu\text{L}$  DMSO) was added to the mAb (3 mg/mL in 1 ml 0.1 M NaHCO<sub>3</sub> buffer, pH 9.0), and incubated for 30 min at 37 °C. Non-conjugated chelator was removed by size exclusion chromatography (SEC) using a PD-10 column and 0.9% sodium chloride solution as eluent.

### 2.6 Determination of chelate-to-mAb ratio

In the coupling of desferrioxamine to the mAb through the N-suc-Df-mAb method, the chelate-to-mAb ratio was monitored *via* UV absorbance of Fe<sup>3+</sup> at 430 nm [21]. Iron was removed by complexation with EDTA before the actual radiolabeling procedure.

In case of the coupling of desferrioxamine to mAb through the Df-Bz-NCS, the chelate-to-mAb molar ratio for rituximab was determined in previous studies [22] following the method described by Meares *et al.* [23]. In short, conjugates were labeled according to the aforementioned procedure with a known nanomolar excess of zirconium oxalate solution spiked with <sup>89</sup>Zr.

### 2.7 Preparation of <sup>90</sup>Nb-labeled N-suc-Df-mAb

N-suc-Df-mAb was labeled with <sup>90</sup>Nb in HEPES buffer at pH 7.0. To <sup>90</sup>Nb (37–50 MBq) in 6 M HCl/0.01 M oxalic acid solution (200  $\mu\text{L}$ ) 6 M NaOH (180  $\mu\text{L}$ ) and afterwards 1 M NaOH (230  $\mu\text{L}$ ) were added to neutralize the acidic

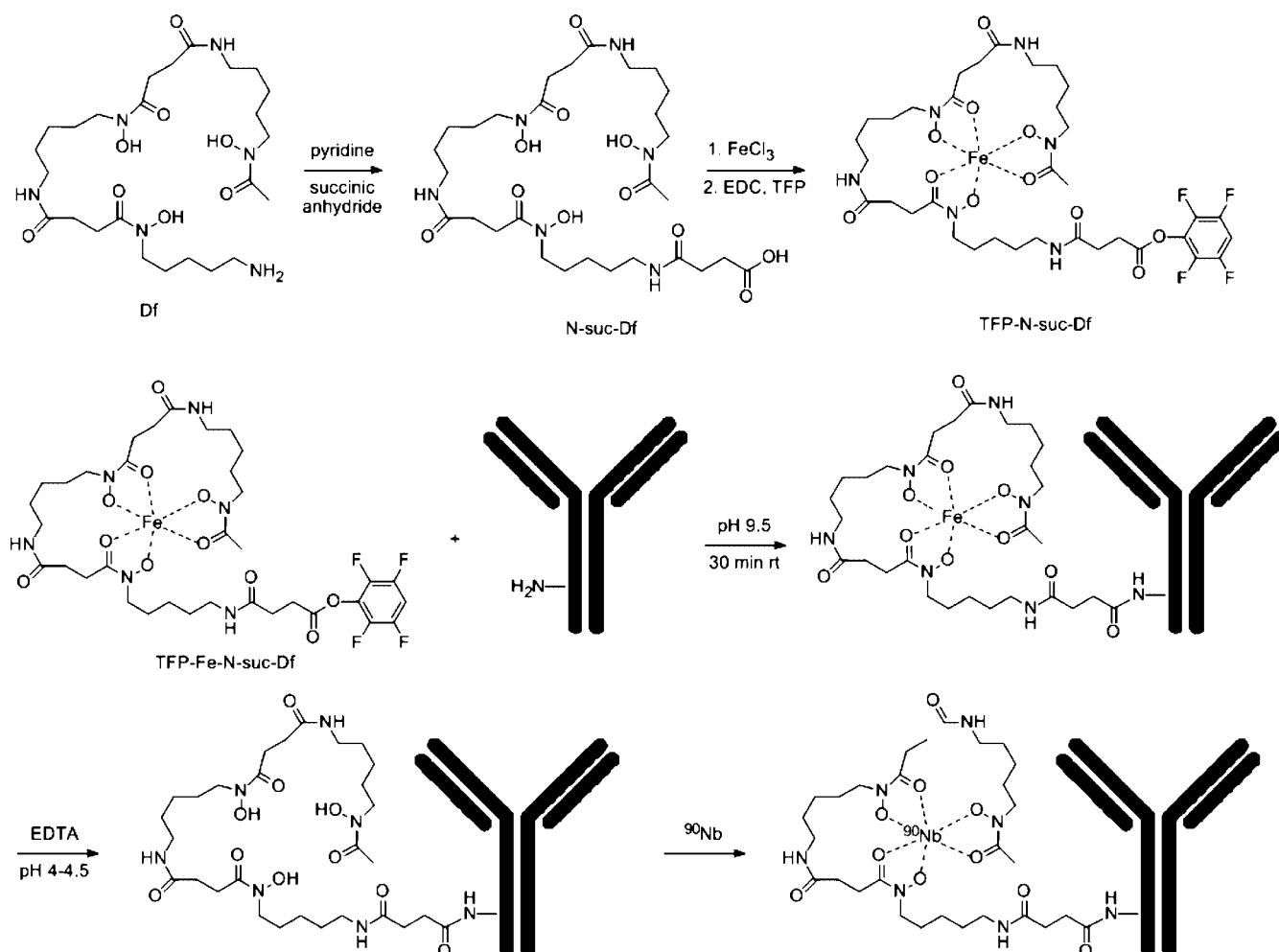


**Fig. 2.** Df-conjugation via TFP-N-suc-Df-Fe and labeling with <sup>90</sup>Nb.

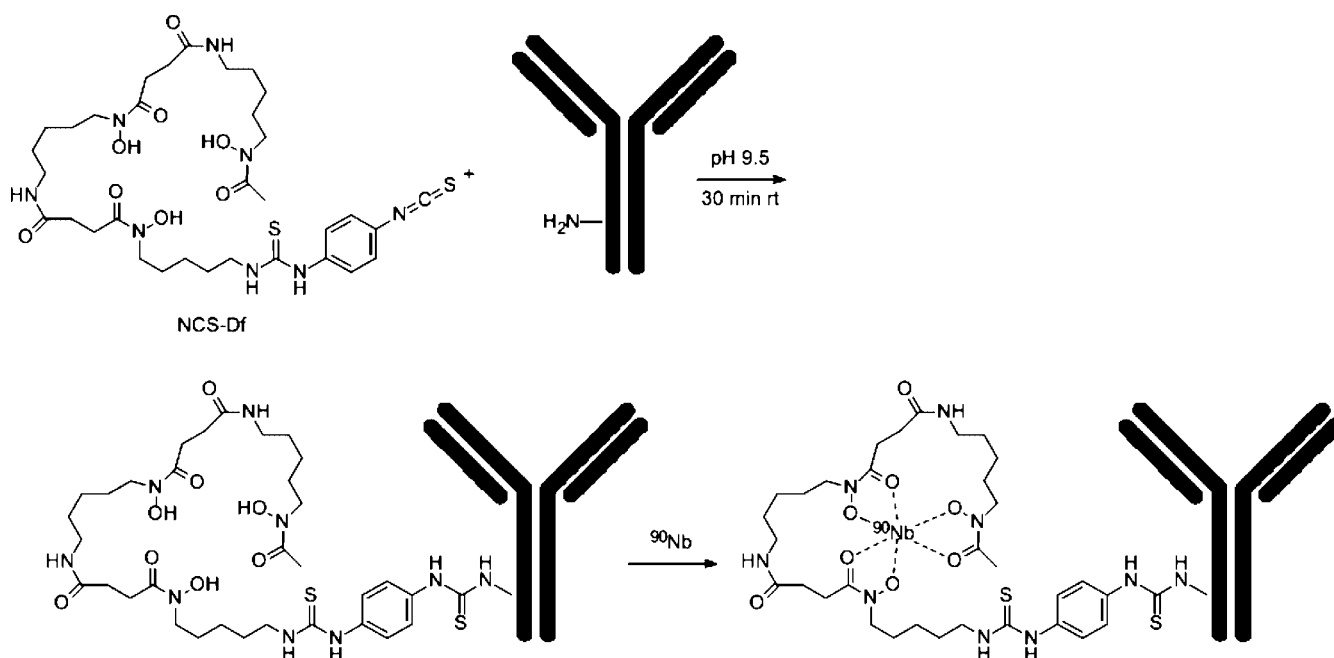


**Fig. 3.** Df-conjugation via the bifunctional chelator Df-Bz-NCS and labeling with <sup>90</sup>Nb.

solution. 0.5 M HEPES buffer (pH 7.0) (300  $\mu$ L), N-suc-Df-mAb (5 mg/mL) (250  $\mu$ L) and 0.5 M HEPES (pH 7.0) (860  $\mu$ L) were added and incubated for 1 h at room tempera-

ture. The overall volume of the reaction mixture was 2 mL. Finally, <sup>90</sup>Nb-N-suc-Df-mAb was purified on a PD-10 column using 0.9% sodium chloride solution as mobile phase.

## 2.8 Preparation of <sup>90</sup>Nb-labeled Df-Bz-NCS-mAb

Df-Bz-NCS-mAb was labeled with <sup>90</sup>Nb at room temperature in a volume of 2 mL under gently stirring for 60 min. To <sup>90</sup>Nb (37–50 MBq) 6 M HCl/0.01 M oxalic acid solution (200  $\mu$ L) 6 M NaOH (180  $\mu$ L) and 1 M NaOH (230  $\mu$ L) were added. 0.5 M HEPES buffer (pH 7.0) (390  $\mu$ L) and Df-Bz-NCS-mAb (1.5 mg/mL) (1.0 mL) were added. Finally, <sup>90</sup>Nb-Df-Bz-NCS-mAb was purified by PD-10 column using a 0.9% sodium chloride solution as mobile phase.

## 2.9 Analytical check of <sup>90</sup>Nb labeling procedures

After each preparation of <sup>90</sup>Nb-labeled Df-Bz-NCS-mAb or N-suc-Df-mAb, the conjugates were analyzed by instant thin-layer chromatography (ITLC), and by high-performance liquid chromatography (HPLC) for radiolabeling efficiency and radiochemical purity. ITLC analyses of <sup>90</sup>Nb-labeled N-suc-Df-mAb or Df-Bz-NCS-mAb was performed on chromatography strips (Biodex, NY). As mobile phase, 0.02 M citrate buffer (pH 5.0) was used. HPLC monitoring of the final products was performed on a Waters HPLC system using a BioSep-SEC-S 2000 size exclusion column (Phenomenex®). As eluent, a mixture of 0.05 M sodium phosphate and 0.15 M sodium chloride (pH 6.8) solution was used at a flow rate of 0.5 mL/min.

## 2.10 *In vitro* stability

Fetal calf serum for stabilities studies was provided by the University Medical Center of the Johannes Gutenberg University Mainz, Germany.

The final activity was adjusted between 15–25 MBq/mL, mAb concentrations varied between 1.25 and 1.5 mg/mL.

For assessing the *in vitro* stability of <sup>90</sup>Nb-Df-Bz-NCS-mAb and <sup>90</sup>Nb-N-suc-Df-mAb, two sets of experiments were performed. In the first set, the labeled mAbs were stored at 4 °C (storage and transportation conditions) in 0.9% sodium chloride solution. At various time points, aliquots were taken and analyzed by ITLC and HPLC.

In a second set, purified radiolabeled mAbs were added to fetal calf serum (FCS) (1 : 4 *v/v* dilution; sodium azide added to 0.02%). The samples were incubated at 37 °C. At various time points, aliquots were taken and analyzed by ITLC and HPLC.

## 3. Results

### 3.1 Production of <sup>90</sup>Nb

The overall irradiation yield of <sup>90</sup>Nb for three 1 h and 5  $\mu$ A irradiations was  $720 \pm 50$  MBq, *i.e.*  $145 \pm 10$  MBq/ $\mu$ A h under given irradiation parameters. The distribution of <sup>90</sup>Nb activity in the 3 foils was: 49%, 40% and 10% for the 1<sup>st</sup>, 2<sup>nd</sup> and 3<sup>rd</sup> foil, respectively. As the third foil got only 10% of the total activity while carrying 1/3 of the mass of the whole target, it may then be eliminated in routine production procedure, in particular to facilitate radiochemical processing. The radionuclidic purity of <sup>90</sup>Nb after EOB was more than 97%. Minor isotopic impurities found were: <sup>92m</sup>Nb( $T_{1/2} = 10.2$  d) = 1.64%, <sup>95</sup>Nb( $T_{1/2} = 35.0$  d) = 0.08%, <sup>95m</sup>Nb( $T_{1/2} = 3.6$  d) = 0.29% and <sup>96</sup>Nb( $T_{1/2} = 23.35$  h) = 0.88%.

### 3.2 Separation and purification of no-carrier added <sup>90</sup>Nb

The extraction steps provided crude separation of <sup>90</sup>Nb from the target material with the organic phase collecting more than 99% of <sup>90</sup>Nb. After the back extraction procedure, the 5 mL aqueous phase contained 90–95% of the <sup>90</sup>Nb activity. After both extractions this corresponds to a high reduction of Zr mass by a factor of  $10^4$ . Subsequent anionic exchange separation further removed traces of Zr. The final separation yield of <sup>90</sup>Nb was 76–81% and the decontamination factor for Zr/Nb was  $\geq 10^7$ , representing  $\leq 26$  ng of Zr present in the final <sup>90</sup>Nb fraction.

### 3.3 Preparation of <sup>90</sup>Nb-labeled N-suc-Df-mAb and <sup>90</sup>Nb-labeled Df-Bz-NCS-mAb

Analysis *via* HPLC showed that TFP-N-suc-Df modification strategies yield about 1.5 molecules of Df per molecule of rituximab. Similar results were obtained also for the NCS-Df modification [22]. For each modification, the <sup>90</sup>Nb labeling yield was  $> 90\%$  (91% ITLC, 94% HPLC) after 1 h. Labeling kinetics indicate that the labeling yields reached 77% already at 15 min and increased to more than 90% after 50 min. After SEC separation on a PD-10 column, the two <sup>90</sup>Nb-Df-mAb derivatives had 99.0% purity. Specific activity of radiolabeled retuxiamb varied between 24.7 and 40 MBq/mg.

### 3.4 *In vitro* stability

For both <sup>90</sup>Nb-labeled mAb derivatives less than 1% of degradation was observed at room temperature in aqueous solution after 18 d. In the presence of fetal calf serum, the <sup>90</sup>Nb-labeled mAbs were more than 95% intact after 5 d and about 90% intact after 9 d.

Differences between the two modification methods were insignificant.

## 4. Discussion

The development of new long-lived *immuno*-PET isotopes is a complex task and requires many factors to be considered: nuclear decay parameters (half-life,  $\beta^+$  energy and branching), production yield, and specific activity, labeling strategies, *in vitro* and *in vivo* stabilities. The medium-long half-life of <sup>90</sup>Nb of 14.6 h makes this isotope particularly suitable for application with antibodies and antibody fragments. Another advantage of <sup>90</sup>Nb is its decay characteristics: relatively high positron branching of 53% and a rather low  $\beta^+$ -energy of  $E_{\text{mean}} = 350$  keV ( $E_{\text{max}} = 1.5$  MeV), which allows high quality PET imaging.

Following our earlier investigations [18–20] on production, separation and labeling chemistry of the new potential *immuno*-PET isotope <sup>90</sup>Nb, the conjugation of <sup>90</sup>Nb to rituximab as a proof of principle monoclonal antibody was investigated.

The excellent production yield of <sup>90</sup>Nb obtained in this study ( $145 \pm 10$  MBq/ $\mu$ A h) is high in comparison with other *immuno*-PET isotopes (<sup>124</sup>I, <sup>89</sup>Zr, <sup>72</sup>As) presented in Table 2, mainly due to its shorter half-life. Furthermore, according to previous studies [18] it may even be enhanced by

**Table 2.** Production yields of a few PET radionuclides [6, 7].

Radionuclide	Commonly used production route	Proton energy range (MeV)	Calculated yield (MBq/ $\mu$ Ah)
$^{124}\text{I}$	$^{124}\text{Te}(p, n)^{124}\text{I}$	12 $\rightarrow$ 8	16
$^{89}\text{Zr}$	$^{89}\text{Y}(p, n)^{89}\text{Zr}$	12 $\rightarrow$ 6	43
$^{72}\text{As}$	$^{\text{nat}}\text{Ge}(p, xn)^{72}\text{As}$	18 $\rightarrow$ 8	93
$^{55}\text{Co}$	$^{58}\text{Ni}(p, \alpha)^{55}\text{Co}$	15 $\rightarrow$ 7	14

a factor of two. Some variation in production yields results from different setups at cyclotron facilities, such as beam parameters, target design and cooling arrangement.

As radiolabeling chemistry of  $^{90}\text{Nb}^{\text{V}}$  appears to be quite similar to that of  $^{89}\text{Zr}^{\text{IV}}$  [21, 22], an almost complete removal of  $\text{Zr}^{\text{IV}}$  from the cyclotron target is essential. A high decontamination factor is crucial, because zirconium also creates very stable complexes with desferrioxamine and competes with niobium, affecting labeling efficiency and causing purity and purification problems. After a multi-step separation procedure, the decontamination factor for  $\text{Zr}/\text{Nb}$  of  $10^7$  was achieved. With 260 mg of  $\text{Zr}$  applied for irradiation this reflects  $\sim 26$  ng of  $\text{Zr}$  remaining after separation.

The separation yield of  $^{90}\text{Nb}$  from metallic  $\text{Zr}$  target varied between 76% and 81%. The whole separation procedure took around 5 h. For routine applications of  $^{90}\text{Nb}$ -labeled compounds, this separation procedure would need to be further optimized to a simpler and faster method.

Labeling of rituximab with  $^{90}\text{Nb}$  was performed *via* the bifunctional chelator desferrioxamine. The monoclonal antibody was successfully modified through two difference methods. The molar ratio for the N-suc-Df method as well as for the Df-Bz-NCS method was 1.5 molecules of desferrioxamine per antibody molecule. Subsequent labeling with  $^{90}\text{Nb}$  showed for both modification strategies the same high yield of more than 90%. *In vitro* stability studies in aqueous solution as well as in the presence of fetal calf serum proved that the  $^{90}\text{Nb}$ -desferrioxamine-antibodies are highly stable over several periods of half-life of  $^{90}\text{Nb}$ , which allows their use in *immuno*-PET.

For future labeling, a modification through the Df-Bz-NCS is preferable for reasons of simpler and faster preparation.

## 5. Conclusions

High production yields and separation efficacies of  $^{90}\text{Nb}$ , high labeling yield procedures for the synthesis of  $^{90}\text{Nb}$ -labeled monoclonal antibodies as well as excellent stability of the  $^{90}\text{Nb}$ -labeled antibody rituximab prove the high potential of  $^{90}\text{Nb}$  as isotope for *immuno*-PET. The high stability of the  $^{90}\text{Nb}$ -Df complexes appears promising for further applications of  $^{90}\text{Nb}$  in combination with biomolecules of intermediate and slow kinetic processes.

*Acknowledgment.* This project was financially supported by the COST action BM0607. The authors thank the teams of TRIGA reactor Mainz for the production of  $^{97}\text{Zr}$  the research reactor BERII at the Helmholtz Center in Berlin for production of  $^{95}\text{Zr}$ , special thanks to Pr. H. Lueddens, the University Medical Center of the Johannes Gutenberg University Mainz, Germany for providing materials for *in vitro* evaluations.

## References

- Wu, A. M., Olafsen, T.: Antibodies for molecular imaging of cancer. *Cancer J.* **14**, 191 (2008).
- US Food and Drug Administration, US Department of Health and Human Services, available from <http://www.fda.gov> (2010).
- Grillo-Lopez, A. J., White, C. A., Dallaire, B. K., Varns, C. L., Shen, C. G., Wei, A., Leonard, J. E., McClure, A., Weaver, L., Cairelli, S., Rosenberg, J.: Rituximab: the first monoclonal antibody approved for the treatment of lymphoma. *Curr. Pharm. Biotechnol.* **1**, 1 (2000).
- van Dongen, G. A. M. S., Visser, G. W. M., Lub-de Hooge, M. N., de Vries, E. G., Perk, L. R.: *Immuno-PET*: A navigator in monoclonal antibody development and applications. *Oncologist* **12**, 1379 (2007).
- Nayak, T. K., Brechbiel, M. W.: Radioimmunoimaging with longer-lived positron-emitting radionuclides: potentials and challenges. *Bioconjug. Chem.* **20**, 825 (2009).
- Qaim, S. M.: Decay data and production yields of some non-standard positron emitters used in PET. *Q. J. Nucl. Med. Mol. Imaging* **52**, 111 (2008).
- Qaim, S. M.: Development of novel positron emitters for medical applications: nuclear and radiochemical aspects. *Radiochim. Acta* **99**, 611 (2011).
- Perk, L. R., Visser, O. J., Stigter-van Walsum, M., Vosjan, M. J. V. D., Visser, G. V. M., Zijlstra, J. M., Huijgens, P. C., van Dongen, G. A. M. S.: Preparation and evaluation of  $^{89}\text{Zr}$ -Zevalin for monitoring of  $^{90}\text{Y}$ -Zevalin biodistribution with positron emission tomography. *Eur. J. Nucl. Med. Mol. Imaging* **33**, 1337 (2006).
- Börjesson, P. K., Jauw, Y. W., Boellaard, R., de Bree, R., Comans, E. F. I., Roos, J. C., Castelijns, J. A., Vosjan, M. J. V. D., Kummer, J. A., Leemans, C. R., Lammerstma, A. A., van Dongen, G. A. M. S.: Performance of immuno-positron emission tomography with zirconium-89-labeled chimeric monoclonal antibody U36 in the detection of lymph node metastases in head and neck cancer patients. *Clin. Canc. Res.* **12**, 2133 (2006).
- Divgi, C. R., Pandit-Taskar, N., Jungbluth, A. A., Reuter, V. E., Goenen, M., Ruan, S., Pierre, C., Nagel, A., Pryma, D. A., Humm, J., Larson, S. M., Old, L. J., Russo, P.: Preoperative characterization of clear-cell renal carcinoma using iodine-124-labelled antibody chimeric G250 ( $^{124}\text{I}$ -cG250) and PET in patients with renal masses: a phase I trial. *Lancet Oncol.* **8**, 304 (2007).
- Deffar, K., Hengliang, S., Liang, L., Wang, X., Zhu, X.: Nanobodies – the new concept in antibody engineering. *African J. Biotechnol.* **8**, 2645 (2009).
- Eder, M., Knackmuss, S., Le Gall, F., Reusch, U., Rybin, V., Little, M., Haberkorn, U., Mier, W., Eisenhut, M.:  $^{68}\text{Ga}$ -labelled recombinant antibody variants for immuno-PET imaging of solid tumours. *Eur. J. Nucl. Med. Mol. Imaging* **37**, 1397 (2010).
- Paudyal, B., Paudyal, P., Oriuchi, N., Hanaoka, H., Tominaga, H., Endo, K.: Positron emission tomography imaging and biodistribution of vascular endothelial growth factor with  $^{64}\text{Cu}$ -labeled bevacizumab in colorectal cancer xenografts. *Cancer Sci.* **102**, 117 (2011).
- Herzog, H., Rösch, F., Stöcklin, G., Lueders, C., Qaim, S. M., Feinendegen, L. E.: Measurement of pharmacokinetics of yttrium-86 radiopharmaceuticals with PET and radiation dose calculation of analogous yttrium-90 radiotherapeutics. *J. Nucl. Med.* **34**, 2222 (1993).
- Rossin, R., Berndorff, D., Friebe, M., Dinkelborg, L. M., Welch, M. J.: Small-animal PET of tumor angiogenesis using a  $^{76}\text{Br}$ -labeled human recombinant antibody fragment to the ED-B domain of fibronectin. *J. Nucl. Med.* **48**, 1172 (2007).
- Browne, E., Firestone, R. B.: *Table of Radioactive Isotopes*. Lawrence Berkeley Laboratory, University of California, Berkeley, CA (1986).
- Qaim, S. M., Bisinger, T., Hilgers, K., Nayak, D., Coenen, H. H.: Positron emission intensities in the decay of  $^{64}\text{Cu}$ ,  $^{76}\text{Br}$  and  $^{124}\text{I}$ . *Radiochim. Acta* **95**, 67 (2007).
- Busse, S., Brockmann, J., Roesch, F.: Radiochemical separation of no-carrier-added radioniobium from zirconium targets for application of  $^{90}\text{Nb}$ -labelled compounds. *Radiochim. Acta* **90**, 411 (2002).

19. Busse, S., Roesch, F., Qaim, S. M.: Cross section data for the production of the positron emitting niobium isotope <sup>90</sup>Nb via the <sup>90</sup>Zr(*p, n*)-reaction. *Radiochim. Acta* **90**, 1 (2002).
20. Busse, S.: Produktion, radiochemische Abtrennung und koordinative Kopplung von <sup>90</sup>Nb zur Synthese potentieller Radiopharmaka für die Positronenemissionstomographie. Ph D. Thesis, University of Mainz (2000).
21. Verel, I., Visser, G. W. M., Boellaard, R., van Walsum, S. M., Snow, G. B., van Dongen, G. A. M. S. <sup>89</sup>Zr *immuno*-PET: comprehensive procedures for the production of <sup>89</sup>Zr-labeled monoclonal antibodies. *J. Nucl. Med.* **44**, 1271 (2003).
22. Perk, L. R., Vosjan, M. J., Visser, G. W., Budde, M., Jurek, P., Kiefer, G. E., van Dongen, G. A. M. S.: *p*-Isothiocyanatobenzyl-desferrioxamine: a new bifunctional chelate for facile radiolabeling of monoclonal antibodies with zirconium-89 for immuno-PET imaging. *Eur. J. Nucl. Med. Mol. Imaging* **37**, 250 (2009).
23. Meares, C. F., McCall, M. J., Reardan, D. T., Goodwin, D. A., Diamanti, C. I., McTigue, M.: Conjugation of antibodies with bifunctional chelating agents: isothiocyanate and bromoacetamide reagents, methods of analysis, and subsequent addition of metal ions. *Anal. Biochem.* **142**, 68 (1984).